OPEN ACCESS
Saudi Journal of Engineering and Technology
Abbreviated Key Title: Saudi J Eng Technol
ISSN 2415-6272 (Print) |ISSN 2415-6264 (Online)
Scholars Middle East Publishers, Dubai, United Arab Emirates
Journal homepage: https://saudijournals.com

Original Research Article

Application of VES and 2D Resistivity Methods for Groundwater Exploration in Kutigi-Enagi Region, Northern Bida Basin, Nigeria

Aweda, A. K.[1,2*], Jatau, B. S.[1], Goki, N. G.[1], Bashir, I. Y[3], Obaje, N. G.[2]

[1]Department of Geology, Nasarawa State University Keffi, Nigeria
[2]Department of Geology, Ibrahim Badamasi Babangida University, Lapai, Nigeria
[3]Department of Geography, Ibrahim Badamasi Babangida University, Lapai, Nigeria

DOI: 10.36348/sjet.2023.v08i02.001 | **Received:** 24.12.2022 | **Accepted:** 03.02.2023 | **Published:** 09.02.2023

***Corresponding author:** Aweda, A. K.
Department of Geology, Nasarawa State University Keffi, Nigeria

Abstract

The study integrates electrical resistivity tomography (ERT) and vertical electrical sounding (VES) methods for investigation of the groundwater potential of the study area. Five ERT was conducted to determine the variation in resistivity of the shallow subsurface rocks both vertically and laterally in order to infer aquifer zones therefrom while twenty-four VES was carried out to compliment the information obtained from the ERT, determine vertical variation in resistivity, infer lateral variation in resistivity, identify depth to aquifer and infer groundwater prospect of the area. Three geoelectric layers were obtained with layer resistivity and thickness increasing northwards with shallower depth to aquifer obtained at Kutigi. K ($\rho1<\rho2>\rho3$) and Q ($\rho1>\rho2>\rho3$) resistivity type curves constitute 75% of obtained curves signifying increasing groundwater saturation and salinity, and are indication of increasing aquifer prospect with depth. The groundwater prospects in the area is generally high with properly constructed boreholes in these areas will produce prolific groundwater at 40 meters with higher yield expected at the southern regions of the study area around Enagi.

Keywords: Aquifer, Bida Basin, Groundwater, ERT, Resistivity.

INTRODUCTION

Groundwater is reported to provide drinking water to at least 50% of the global population and accounts for 43% of all water used for irrigation (Hölting and Coldewery, 2018). Though groundwater is a dynamic and replenishable resource, it is controlled by different hydrogeological, geological and geomorphological conditions (Harini *et al.*, 2018). However, it is generally potable at source and has a low temporal variability making it almost the only source of water for rural communities (Nyagwambo, 2006). Groundwater development is complicated by highly variable hydrogeological conditions rendering its management fraught with uncertainty (Taylor and Barrett, 1999).

Geophysical methods have been used for groundwater exploration and aquifer delineation and are increasingly becoming more relevant in a wide variety of hydrological and hydrogeological investigation because they provide reliable information on the spatial distribution of the physical properties of subsurface features quickly at low cost with minimal or no disturbance to the environment.

Vertical electrical sounding (VES) and horizontal profiling are traditionally the most common electrical resistivity method used in groundwater exploration. However, electrical resistivity tomography (ERT) has recently become increasingly common in groundwater exploration especially in areas with complex geology (Nyagwambo, 2006). Unlike the 1D–VES survey that provides only layered model structures for the subsurface; the ERT method provides both vertical and lateral variation in resistivity thereby making it possible to determine sedimentary facie changes. Ewusi *et al.*, (2009) demonstrated the advantage of the ERT technique over the conventional 1D–VES in groundwater exploration in a sedimentary basin. Drilling success was upgraded to 60% as against 38% for VES within the mudstone and shale formations of the basin. Aizeboekhai *et al.*, (2016) integrated ERT imaging with VES and chargeability to delineate groundwater potential zones in parts of the Dahomey Basin, southwestern Nigeria. The ERT inverse models

were able to delineate the aquifers and the aquitard laterally and also the aquifer thickness as well as depth to aquifer. This method was used to determine the geological contact between the red mudstone and the sandstone zone of Kedah in the work of NurAmalina (2017). Interpretation of VES data by Hewaidy *et al.*, (2015) in the northwestern part of the Gulf of Suez correlated perfectly with logs obtained from a borehole within the area indicating the efficiency of the geophysical method for studying subsurface lithologies in sedimentary basins. Boubaya (2017) integrated electrical sounding (VES), magnetic data and hydrogeological data in an attempt to demonstrate the importance of integrated methods in delineation of deep aquifers in the Maghnia plain. The validity of the hydrogeological interpretation of the geophysical data is proved by several agreements between the resistivity distribution with depth and the aquifer characteristics.

The study area has recently witnessed higher demand and pressure on groundwater resources from boreholes and wells as a result of ongoing oil exploration in the Bida Basin which has resulted to increase in human population. Thus, making provision of clean and sustainable water provision to meet domestic supply is increasingly under threat. Siting of water wells within the area has been done mainly based on recommendations from vertical electrical sounding (VES). The exercise has resulted in random success, with average borehole success rate not more than fifty percent (50%). Idris-Nda *et al.*, (2014) has classified this area as being hydrogeologically complex with low groundwater yield to boreholes. This research presents an integration of ERT and VES methods in an attempt to identify the aquifers in the area, their depth, thickness and delineate the most prospective areas for water well siting in the study area to meet the growing demand for groundwater.

The Study Area and Description

Location, Climate and Topography

Enagi – Kutigi area lies between Latitude 9º7'N to 9º12'N and Longitude 5º32'E to 5º36'E (Figure 1). It is located within the northern Bida Basin of Nigeria and has an estimated population of about 50,000 inhabitants. Its inhabitants are mainly agrarians that rely on groundwater especially for agricultural activities and human consumption. The area is part of the southern Guinea Savannah climate zone of Nigeria with mean annual rainfall of 100mm and mean yearly temperature of 30°C. It has a hilly topography in most part with surface elevation of between 277 m and 161 m above sea level. The main streams are flowing in the southwest and northeast direction respectively with a dendritic pattern.

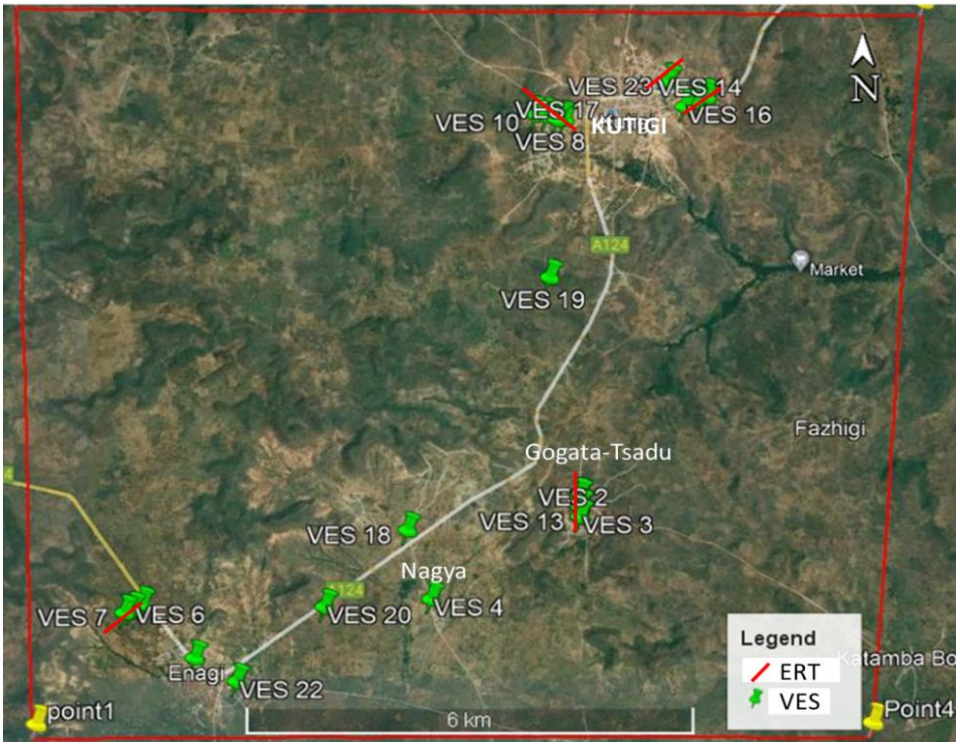

Figure 1: Data Collection Layout in the Study Area

Geology and Hydrogeology

The study area is part of the NW-SE trending intracratonoc Bida Basin which stretches northwards from the Niger-Benue River confluence at Lokoja to the basement complex which marks its northwest extent, separating it from the Sokoto Basin (Rahaman *et al.*, 2019). Various authors (Adeleye, 1974; Kogbe, 1989; Obaje, 2009; Rahaman *et al.*, 2019) have studied the regional geology of the Bida Basin in details. The geological map of the area is shown in Figure 2.

Outcropping sections of rocks from the Bida and Enagi formations is predominate in the study area. The Bida Formation is composed of a basal conglomeratic sandstone and fines upward into medium-grained sandstone, siltstone and subordinate claystone, covering about 40% of the study area. The Sakpe Formation, which account for roughly 10% of the study area, outcrops in the southeastern part and is predominantly oolitic and pisolitic ironstone band, sandwiching a silt to mudstone unit with concretions at the top. The Enagi Formation outcrops dominantly in the northwest areas accounting for about 50% of the underlying geology. Its lithology comprises of a coarsening upward sequence of clayey siltstone and sandstone.

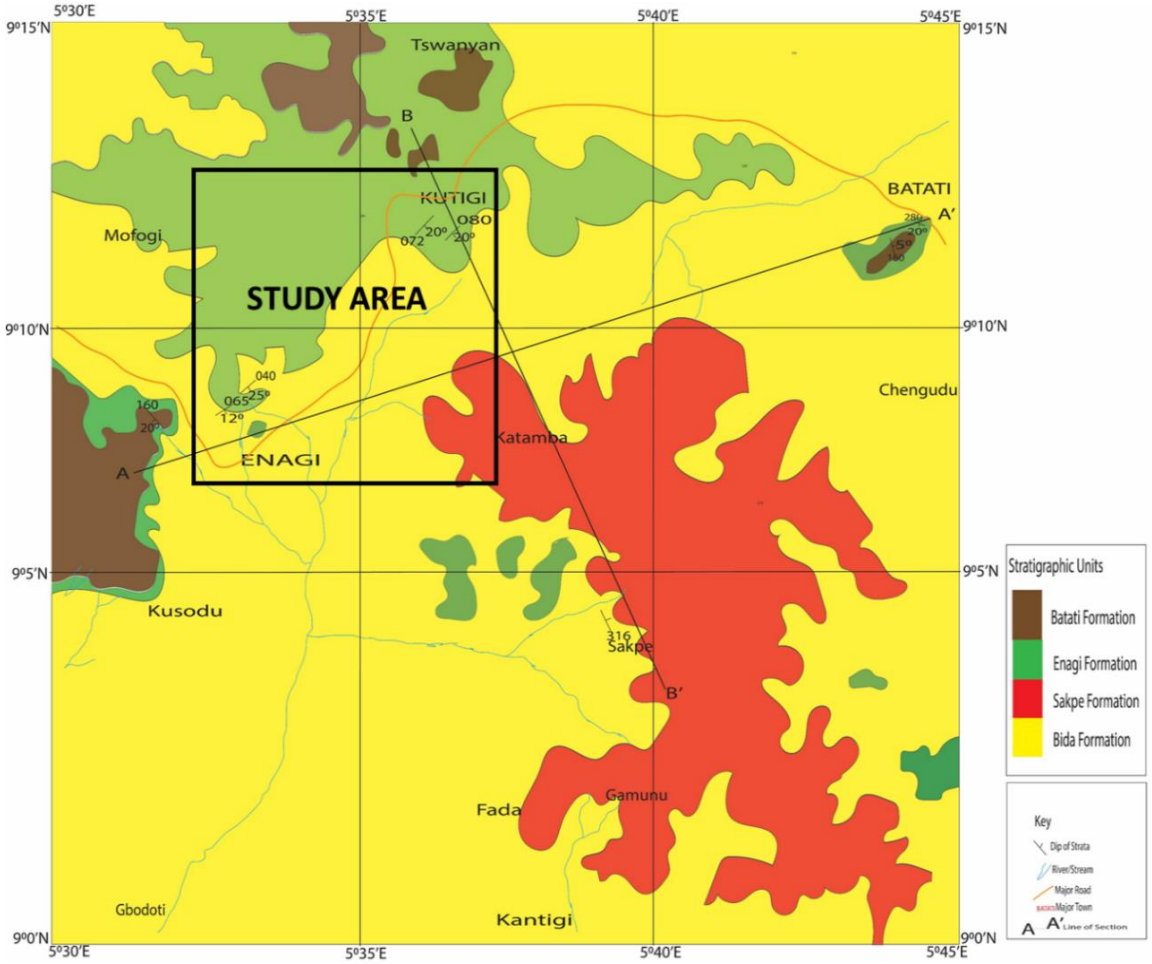

Figure 2: Geological Map of the Study Area

The study area is part of the Lower Niger Hydrological Basin which is believed to have low to moderate groundwater. The sandstone intervals in the various formations are believed to be potentially good aquifer even though groundwater development records are rarely available. The major aquifer units in the Northern Bida Basin are the Bida Sandstone and the alluvial deposits. The Bida Sandstone aquifer units are composed of very poorly sorted pebbly arkoses, sub-arkoses and quartzose sandstones (Obaje, 2009). Olabode *et al.,* (2012) reported aquifer yield between 0.9 m^3/hr and 136.5 m^3/hr during pump test of water wells within the Bida Sansdstone and average transmissivity values between 1.365 m^3/day and 393m^3/day as computed using Jacob and Theis' methods. The alluvial aquifer, which invariably overlies the sandstone aquifer in some places, is recharged directly by rainfall or the adjoining flood waters of the river systems. It has thickness of up to 30m in some places and sustains considerable subsurface groundwater flow.

METHODOLOGY

Resistivity Method

Five ERT profiles of 300 meters were covered using the Wenner (alpha) configuration and inter-electrode spacing of 10 meters to ensure high resolution at the required depth of investigation (Figure 1). Wenner method is preferred because it has a very high signal strength and good signal to noise ratio, allowing for acquisition of high resolution 2D ERT data in addition to having more vertical sensitivity and great depth of investigation. Profiles were selected such that most of them run across existing boreholes and as such, ensuring correlation with already existing data. ERT prospecting is conducted by using an array of electrodes equally spaced along a profile (Figure 3), allowing the production of a very detailed subsurface image in the

form of a pseudo-section which results from estimation of a large number of resistivity values at varying depths along the investigated profile (or area) (Rani, 2017). The apparent resistivity was obtained by multiplying the resistance with the geometric factor; K = (2πa) where is the electrode spacing.

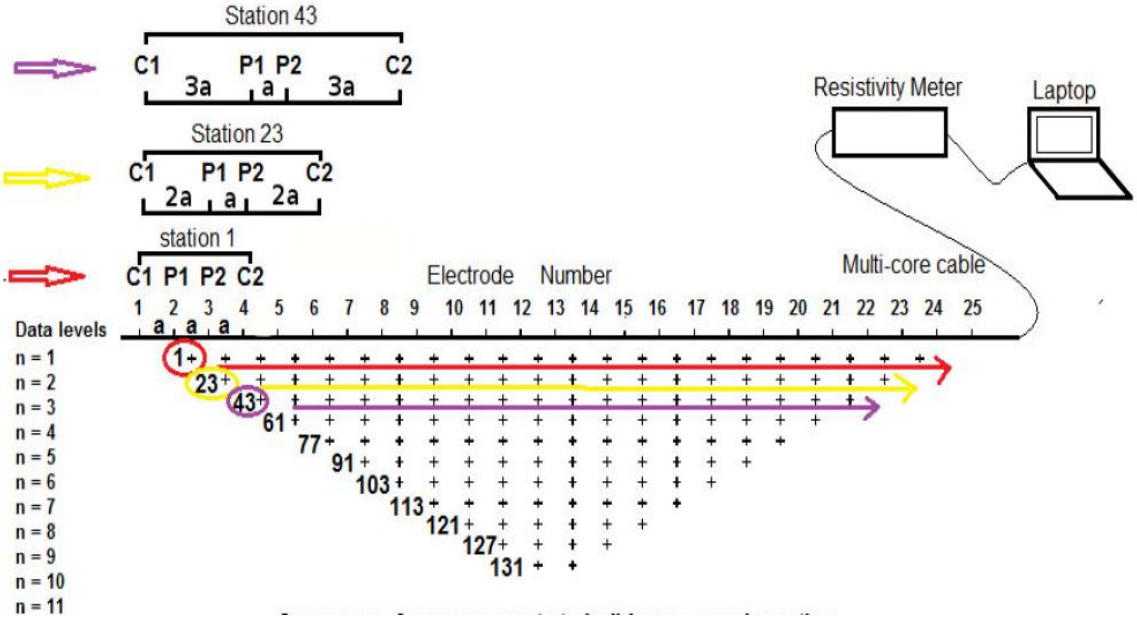

Figure 3: ERT Data Measurement Sequence (After Sikah *et al.*, 2016)

Twenty-four VES points were sounded at 0, 150 and 300 meters along the ERT profile as well as in other locations where the ERT could not be deployed (Figure 1). In this method, the mid-point of the array is fixed while the electrodes are moved at the opposite sides of the array (Figure 1). This yielded the vertical variations in the subsurface resistivity distribution about the mid-point of the entire electrode spread. A half-current electrode spacing (AB/2) of 200 meters was used for the data measurement of the resistivity sounding. The electrode spread used for the soundings was considered sufficient for the effective depth of investigation anticipated. The apparent resistivity was obtained by multiplying the resistivity reading obtained by the calculated geometric factor (K) determined using the formulae;

$$K = \pi\left(\frac{\left(\frac{AB}{2}\right)^2 - \left(\frac{MN}{2}\right)^2}{2\left(\frac{MN}{2}\right)}\right)$$

The obtained ERT dataset were processed and inverted concurrently using a tomography inversion scheme RES2DINV to obtain true resistivity profiles (Loke and Barker, 1996). The program uses a non-linear optimization technique that automatically determines the inverse model of the 2D resistivity of the subsurface for the measured apparent resistivity and divides the subsurface into a number of rectangular blocks according to the spread and density of the observed area. The survey parameters (electrode configuration, electrode separations and positions, and data level) used for the data measurements determines the size and number of the blocks. Least-squares inversion technique with standard least-squares constraint (L2- norm or smoothness), which minimizes the square of the difference between the observed and the computed apparent resistivity was used for the data inversion. The data was processed with four to six iterations when the data produced more logical and realistic geological models with low RMS error (1.6 – 14.3%). Topography data were included in the data prior to inversion so that the depth in the resistivity model is referenced to mean seal level. The VES data was interpreted by plotting the apparent resistivity against electrode spacing using curve matching with the master curve and the WinResist software. The curves were classified based on their shapes and related to their indication for groundwater.

RESULTS AND DISCUSSIONS

In the interpretation of the resistivity pseudo-section, the vertical and lateral subsurface resistivity is considered along the survey line (Khaki *et al.*, 2016). For the ERT pseudo-section, caption I present the apparent resistivity pseudo- section which is the actual data obtained on the field as inputted into the software; II is the calculated apparent resistivity pseudo-section which is a synthetic model used to estimate the pixel sizes at different layers; III is the inverse model which represents the geo-electric section and is a close representation of the true geologic model of the subsurface (Figure 4).

The pseudo-sections consist of three layers. The first layer has an apparent resistivity of 300 to 8200Ωm which consists of highly indurated clays and

silt. The resistivity of this layer is lowest southwards around Enagi and increases towards Kutigi, where it is highest. This is attributed to the increased ferruginization of the claystones and siltstone around Kutigi which makes them highly resistive. The thickness of this layer is between 5 meters and 10 meters with greater layer thickness observed at Kutigi. The second layer is a less resistive layer with resistivity range of 90Ωm and 150Ωm which is interpreted as a slightly saturated sandy to silty clay layer, with saturation increasing with depth. This layer is present from depth of 5 meters around Enagi and 15.4 meters in Kutigi. The thickness of this layer is greater in Enagi (25 meters) and is shallower at Kutigi (10 meters). The thin sand intervals of this layer provide groundwater supply to hand dug wells whose depth rarely exceeds 15 meters. The third layer consists of aquiferous clayey sands with lower resistivity range in comparison to the other two layers, which also reflects its possible high saturation. It has an apparent resistivity range of 13 Ωm and 589 Ωm with least values obtained around Enagi, where it is pebbly, signifying possible higher saturation of the aquifer. This layer occurs from about 25 meters in Enagi and increases gently to depth of around 30 meters depth in Kutgi.

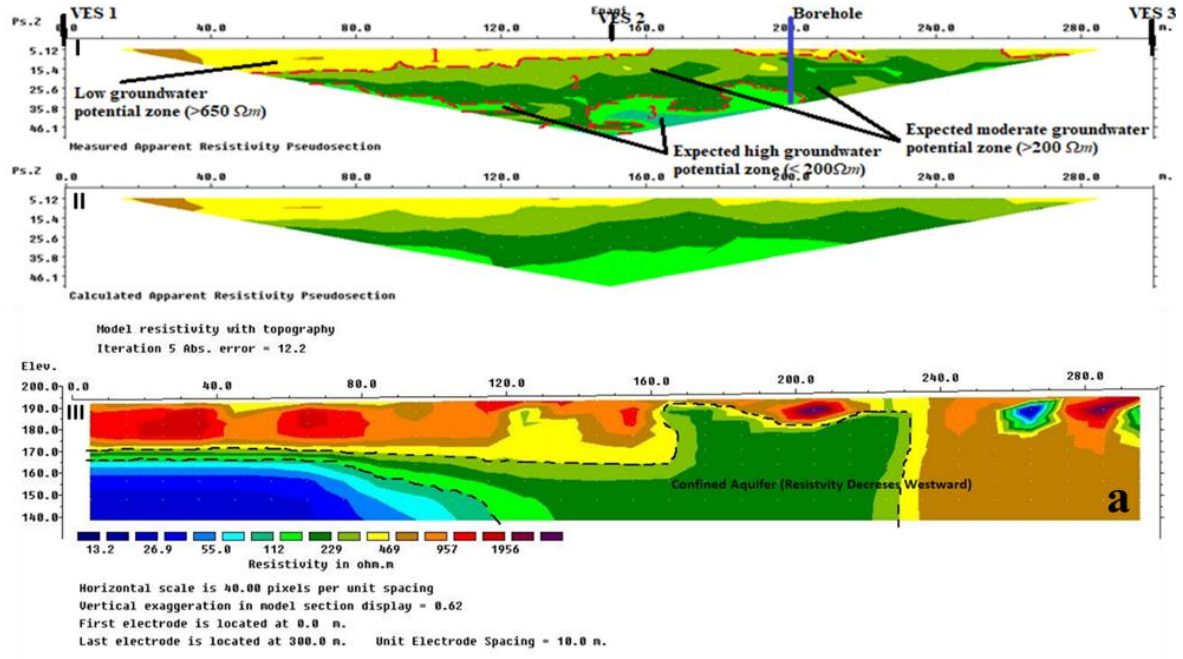

a

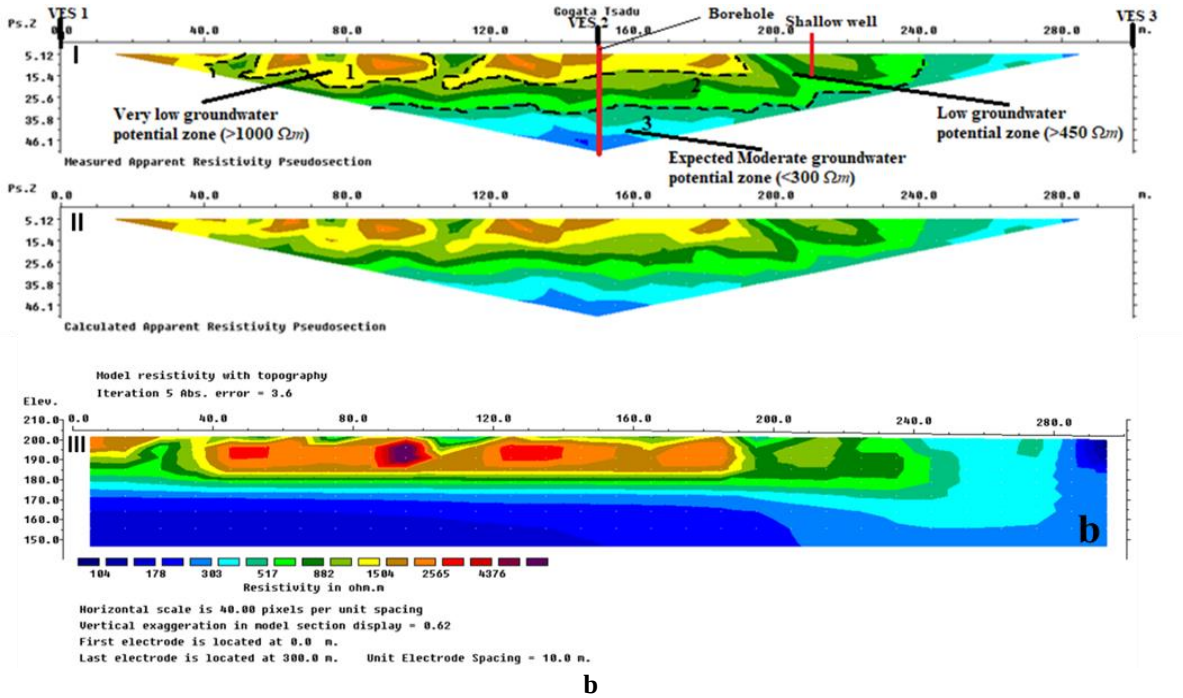

b

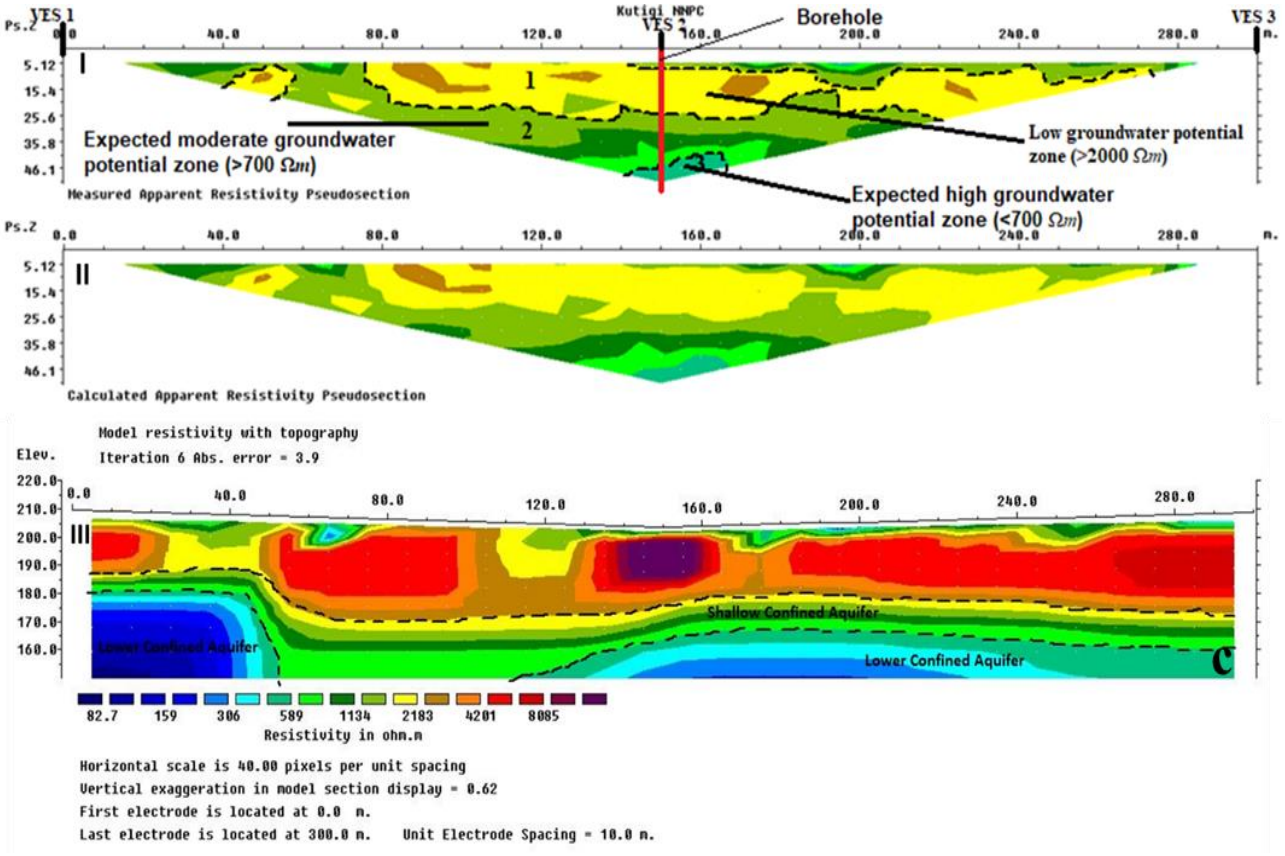
VES 1
Kutigi NNPC
VES 2
Borehole
VES 3
Expected moderate groundwater potential zone (>700 Ωm)
Low groundwater potential zone (>2000 Ωm)
Expected high groundwater potential zone (<700 Ωm)
Measured Apparent Resistivity Pseudosection
Calculated Apparent Resistivity Pseudosection
Model resistivity with topography
Iteration 6 Abs. error = 3.9
Elev.
Shallow Confined Aquifer
Lower Confined Aquifer
c
82.7 159 306 589 1134 2183 4201 8085
Resistivity in ohm.m
Horizontal scale is 40.00 pixels per unit spacing
Vertical exaggeration in model section display = 0.62
First electrode is located at 0.0 m.
Last electrode is located at 300.0 m. Unit Electrode Spacing = 10.0 m.

c

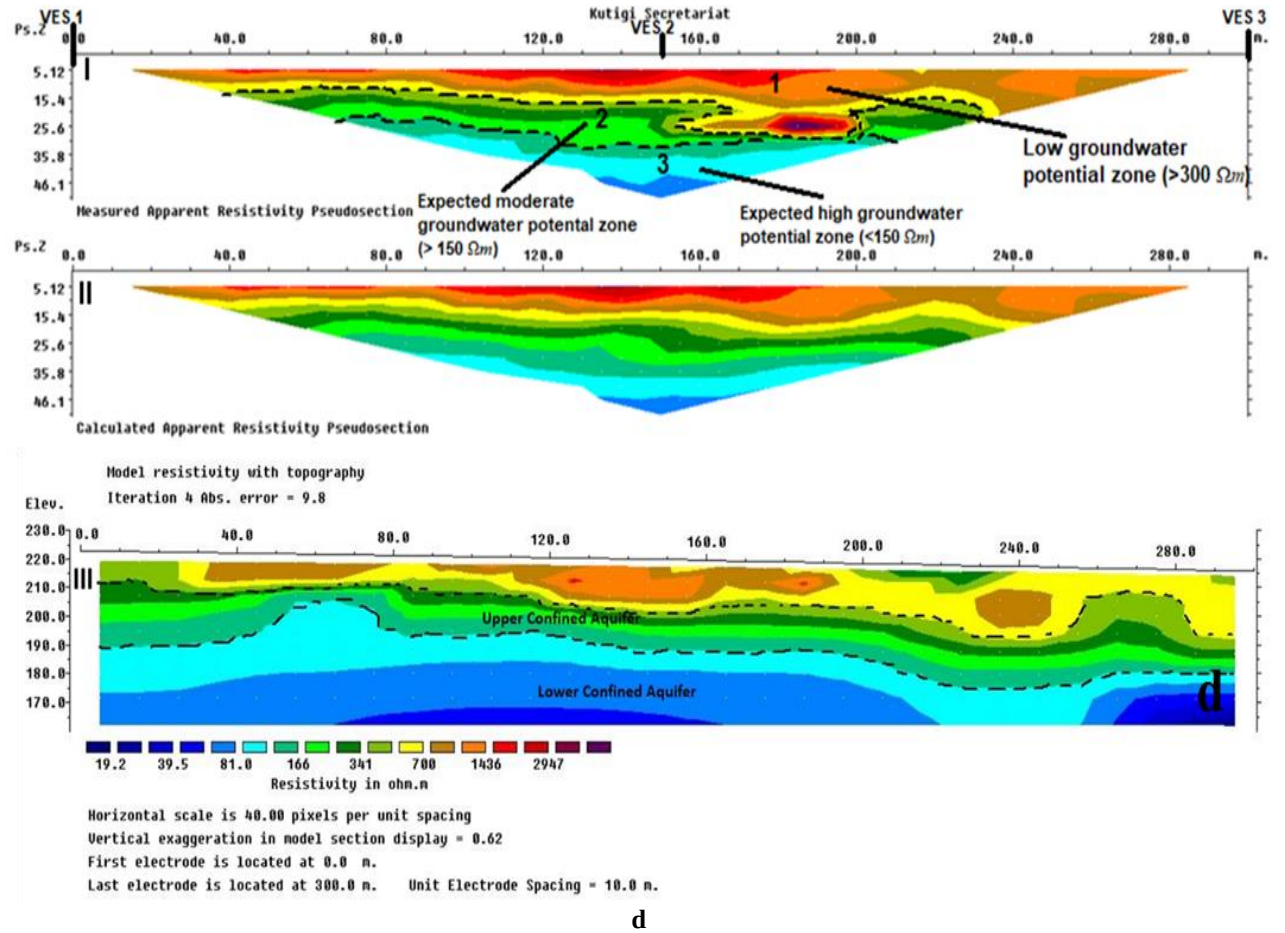
VES 1
Kutigi Secretariat
VES 2
VES 3
Low groundwater potential zone (>300 Ωm)
Expected moderate groundwater potential zone (> 150 Ωm)
Expected high groundwater potential zone (<150 Ωm)
Measured Apparent Resistivity Pseudosection
Calculated Apparent Resistivity Pseudosection
Model resistivity with topography
Iteration 4 Abs. error = 9.8
Elev.
Upper Confined Aquifer
Lower Confined Aquifer
d
19.2 39.5 81.0 166 341 700 1436 2947
Resistivity in ohm.m
Horizontal scale is 40.00 pixels per unit spacing
Vertical exaggeration in model section display = 0.62
First electrode is located at 0.0 m.
Last electrode is located at 300.0 m. Unit Electrode Spacing = 10.0 m.

d

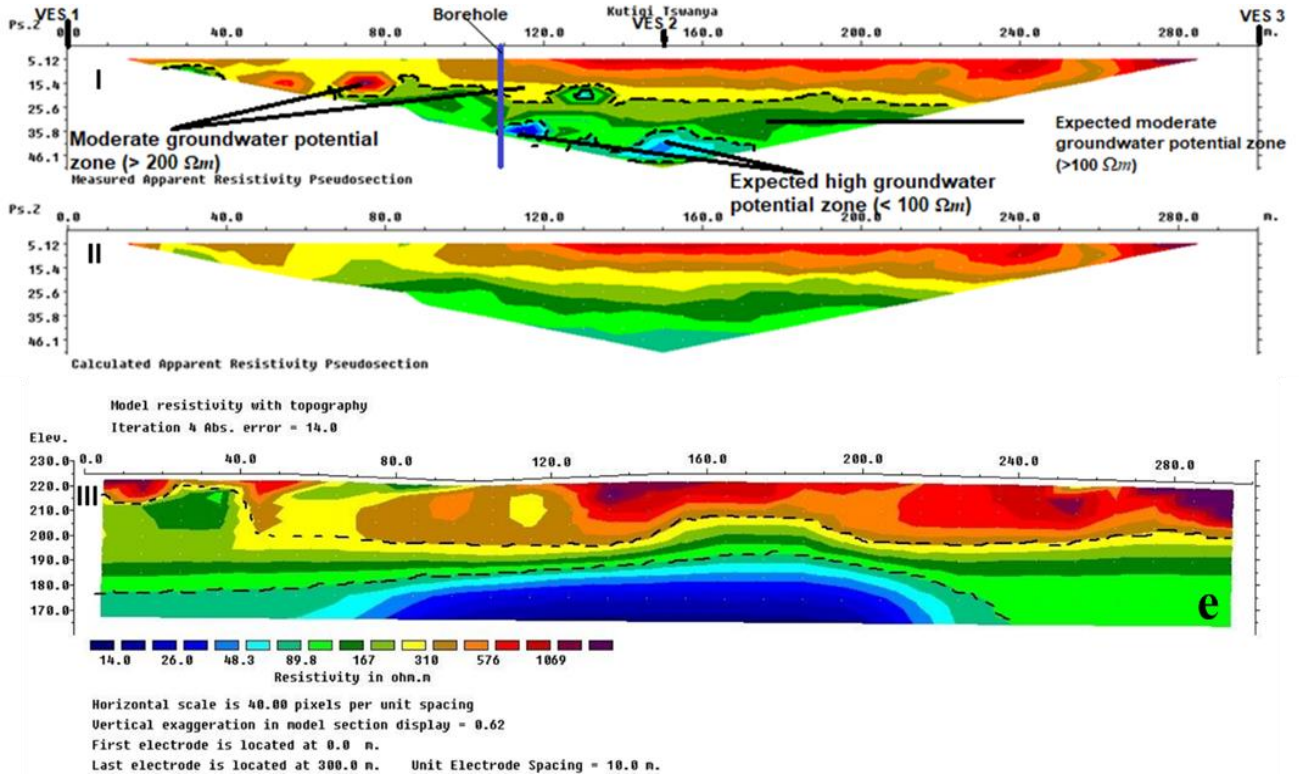

Figure 4 (a-e): Measured, Calculated and Inverse Resistivity Models from the Study Area

The inverse resistivity model was correlated with a borehole lithologic log obtained from Kutigi as this is a useful way of obtaining a realistic interpretation of the resistivity profile (Khaki *et al.*, 2016). The result of the comparison showed a match between the resistivity and the lithofacies obtained from the borehole log (Figure 5). The high apparent resistivity values of 400Ωm-1100Ωm obtained at 0meter to 25meters depth correspond to compacted fine to coarse sands, sandy clay and gravely clay which are not fully saturated. Lower resistivity values of 89.8Ωm to 167Ωm correspond to intercalations of saturated clayey sand and gravely clayey sand while resistivity values of less than 89.8Ωm represent saturated sandy clays and clayey pebbly sands.

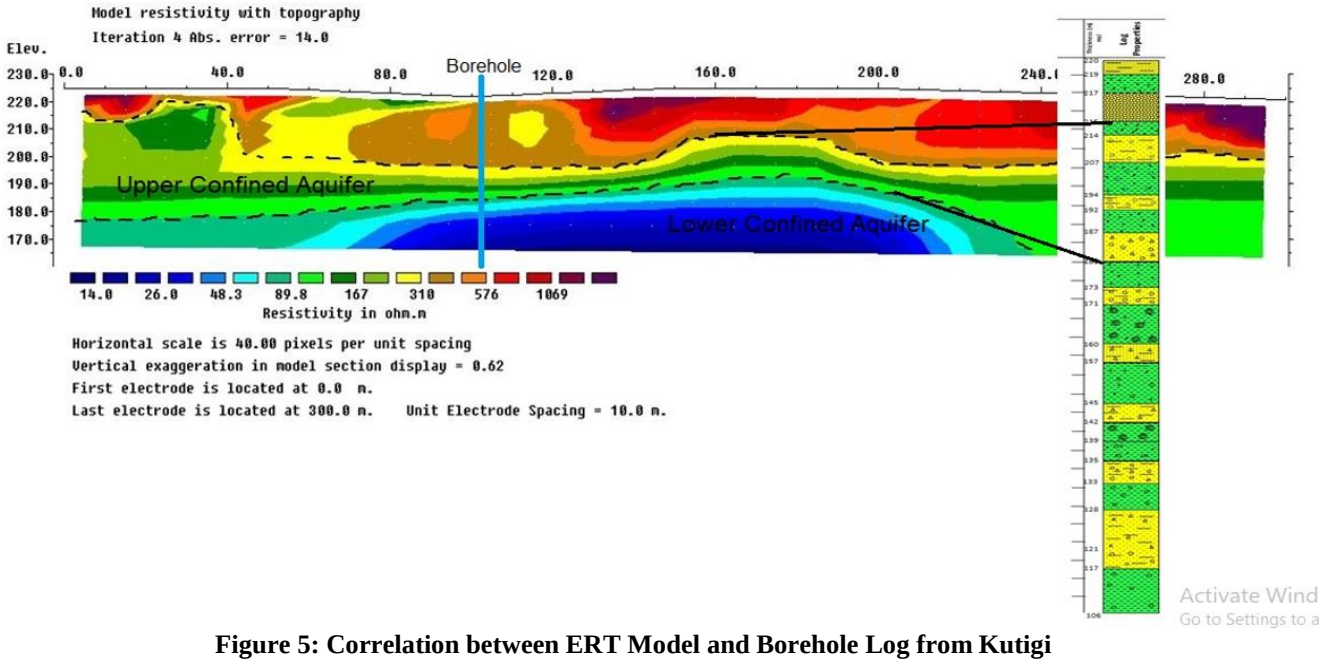

Figure 5: Correlation between ERT Model and Borehole Log from Kutigi

The Vertical electrical sounding (VES) was deployed to study the aquifers at greater depth especially since the ERT could not investigate more than 60 meters depth. Three VES stations were located at the extremes and middle of each ERT profiles to assess at greater depth, the lateral variation of resistivity with depth and infer the various lithologies and integrate these with the ERT profiles to delineate the various aquifers within the study area. The plot of apparent resistivity against AB/2 were curve matched using the Schlumberger master curve and plotted using the 1D inverse resistivity software, WIRESIST, from which the curve types and number of layers present were delineated. An example inverse type curve is presented in Figure 6. The area is characterized by three to four lithological layers (Table 1-3), with the top layer characterized as silty to sandy soil and ferruginized clay soil which is highly resistive. Other subsurface layers are sand to silty clay and aquiferous clayey sand which is pebbly around Enagi.

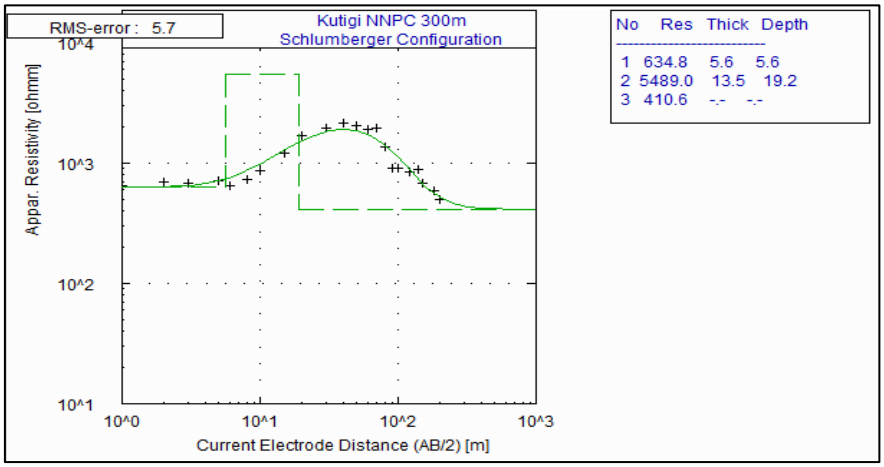

Figure 6: Resistivity Type curve for VES 16

The summary table of the resistivity curve types interpreted for the sounded locations is presented in Table 2. The K-type curve (ρ1<ρ2>ρ3) is the most dominant (41.7%) curve type and was obtained dominantly in the northern part of the study area especially around Kutigi. These curves indicate slight increase and then decrease in resistivity with depth which is an indication of increasing groundwater saturation and salinity, and are indication of increasing aquifer prospect with depth. The curve type changes into HK, KH, QH and Q westwards towards Enagi. The Q (ρ1>ρ2>ρ3) and QH-type curves (ρ1>ρ2>ρ3<ρ4), which is about 37.5% of all curve types is the dominant curve type in the southern sector of the study area. This curve generally depicts a situation of continuous decrease in resistivity with depth which represents shallow aquifers in areas such as the study area. The HK-type curve (ρ1>ρ2<ρ3>ρ4) which is interpreted around Gogata-Tsadu depicts the presence of a ferruginized clay layer overlying the clayey sand aquifers and constitutes 12.5% of the curve types.

Table 1: Geo-electrical Table for VES 1-9

VES	Location	Curve Type	No. of Layers	Layer Resistivity	Resistivity Model	Layer Thickness	Layer Depth	Inferred Lithology
1	K-Tswanya 0	Q	3	554.5	ρ1>ρ2>ρ3	1	1	Sandy Top Soil
				302.9		43.6	44.6	Silty to Sandy Clay
				13.3		∞	∞	Clayey Sand
2	K-Tswaya 150	Q	3	603.6	ρ1>ρ2>ρ3	1.1	1.1	Sandy Top Soil
				335.7		43.5	44.6	Silty to Sandy Clay
				15.3		∞	∞	Clayey Sand
3	K-Tswanya 300	K	3	400.8	ρ1<ρ2>ρ3	2.2	2.2	Sandy Top Soil
				549.8		21.6	23.8	Silty to Sandy Clay
				55.6		∞	∞	Clayey Sand
4	Nagya	Q	3	387.6	ρ1>ρ2>ρ3	1.8	1.8	Sandy Top Soil
				195.3		41.5	43.4	Silty to Sandy Clay
				33.5		∞	∞	Clayey Pebbly Sand
5	Enagi 0	Q	3	914.3	ρ1>ρ2>ρ3	1.1	1.1	Sandy Top Soil
				517.5		28	28.1	Silty to Sandy Clay
				78.8		∞	∞	Pebbly Clayey Sand
6	Enagi 150	Q	3	787.5	ρ1>ρ2>ρ3	3	3	Sandy Top Soil
				971.3		25.2	28.2	Silty to Sandy Clay
				101.6		∞	∞	Pebbly Clayey Sand
7	Enagi 300	Q	3	806.2	ρ1>ρ2>ρ3	2.8	2.8	Sandy Top Soil
				856.6		20.8	23.6	Silty to Sandy Clay

VES	Location	Curve Type	No. of Layers	Layer Resistivity	Resistivity Model	Layer Thickness	Layer Depth	Inferred Lithology
				109		∞	∞	Pebbly Clayey Sand
8	K-Sec 0	K	3	451.1	ρ1<ρ2>ρ3	2.2	2.2	Sandy Top Soil
				897.9		16.7	18.9	Silty to Sandy Clay
				54.2		∞	∞	Clayey Sand
9	K-Sec 150	K	3	484.7	ρ1<ρ2>ρ3	2.4	2.4	Sandy Top Soil
				1046		15.2	17.6	Silty to Sandy Clay
				61.4		∞	∞	Clayey Sand

Table 2: Geo-electrical Table for VES 10-20

VES	Location	CURVE TYPE	No. of Layers	Layer Resistivity	Resistivity Model	Layer Thickness	Layer Depth	Inferred Lithology
10	K-Sec 300	K	3	186.8	ρ1<ρ2>ρ3	1.9	1.9	Sandy Top Soil
				539.1		22.3	24.2	Silty to Sandy Clay
				74.2		∞	∞	Clayey Sand
11	G-Tsadu 0	HK	4	668.3	ρ1>ρ2<ρ3>ρ4	1.1	1.1	Sandy Top Soil
				376.7		1.5	2.6	Ferruginized Clay
				714.1		20.9	23.4	Clayey Sand
				78.7		∞	∞	Silty Sand
12	G-Tsadu 150	HK	4	1135.1	ρ1>ρ2<ρ3>ρ4	0.9	0.9	Sandy Top Soil
				701.7		2	2.9	Ferruginized Clay
				1216.8		20.3	23.2	Clayey Sand
				131.4		∞	∞	Clayey to Silty Sand
13	G-Tsadu 300	HK	4	353.8	ρ1>ρ2<ρ3>ρ4	1.9	1.9	Sandy Top Soil
				131.1		11.1	13.1	Ferruginized Clay
				259.9		31.4	44.4	Clayey Sand
				87.9		∞	∞	Clayey to Silty Sand
14	K-NNPC 0	K	3	428.5	ρ1<ρ2>ρ3	8.7	8.7	Ferruginized Clay
				1642.3		18.8	27.5	Sandy Clay
				209.7		∞	∞	Clayey Sand
15	K-NNPC 150	K	3	533.4	ρ1<ρ2>ρ3	9.1	9.1	Ferruginized Clay
				2260.5		18.4	27.5	Sandy Clay
				223.8		∞	∞	Clayey Sand
16	K-NNPC 300	K	3	634.8	ρ1<ρ2>ρ3	5.6	5.6	Ferruginized Clay
				5489		13.5	19.2	Sandy Clay
				410.6		∞	∞	Clayey Sand
17	Kutigi C	K	4	171.5	ρ1<ρ2>ρ3	9	9	Sandy Top Soil
				796.4		35.7	44.7	Sandy Clay
				357.9		∞	∞	Clayey Sand
18	Kutigi CAIS	KH	4	1749	ρ1<ρ2>ρ3>ρ4	4.1	4.1	Silty Sand Top Soil
				4901.5		8.5	12.6	Ferruginized Clay
				2197.1		24.5	37.1	Sandy Clay
				1459.1		∞	∞	Clayey Sand
19	Bokungi	K	3	193.4	ρ1<ρ2>ρ3	2.2	2.2	Clayey Top Soil
				393.4		27.3	29.5	Sandy Clay
				372		∞	∞	Clayey Sand
20	Safo	Q	3	703.5	ρ1>ρ2>ρ3	3.1	3.1	Clayey Top Soil
				250.7		38.7	41.8	Sandy Clay
				50.4		∞	∞	Clayey Sand

Table 3: Geo-electrical Table for VES 21-24

VES	Location	CURVE TYPE	No. of Layers	Layer Resistivity	Resistivity Model	Layer Thickness	Layer Depth	Inferred Litholohy
21	Enagi CAIS	QH	4	1205.8	ρ1>ρ2>ρ3<ρ4	0.8	0.8	Sandy Top Soil
				271.6		2.3	3.1	Silty Clay
				107		31.5	34.6	Sandy Clay
				400.9		∞	∞	Pebbly Clayey Sand
22	Enagi Pri Sch	Q	3	502.7	ρ1>ρ2>ρ3	1.5	1.5	Sandy Top Soil
				150.3		35.7	37.2	Sandy Clay
				24.6		∞	∞	Pebbly Clayey Sand
23	Enagi Sec	KH	4	184.9	ρ1<ρ2>ρ3<ρ4	5.2	5.2	Sandy Top Soil
				501.2		6.7	11.9	Silty Clay
				214.6		32.1	44	Sandy Clay
				326.9		∞	∞	Pebbly Clayey Sand
24	Kutigi Pri Sch	K	3	141.7	ρ1<ρ2>ρ3	5.3	5.3	Sandy Top Soil
				170.3		26.7	32	Sandy Clay
				126.9		∞	∞	Pebbly Clayey Sand

Table 4: Summary Table of Resistivity Curve Types

Curve Type	Frequency	Dominant Locations
K	10	Kutigi
Q	8	Enagi, Safo, Tswanya
HK	3	Gogata
KH	2	Enagi, Kut CAIS
QH	1	Enagi CAIS

Interpreting the geoelectrical section across the study area (Figure 7) revealed a general decrease in layer resistivity from north to south. The sandy clay layer overlying and confining the clayey sand aquifer also gets thicker in this direction, with a layer thickness of about 25 meters compared to a thickness of 8 meters in the north. The depth to aquifer is shallower at the north with depth to aquifer of about 20 meters around Kutigi. The geoelectric section interpreted from this area correlates with the borehole log (Figure 7) collected from the study area. The aquifer resistivity (Figure 8) is also higher around Kutigi with resistivity value of 400Ωm. The high value is possibly as a result of the presence of ferruginized clay noodles in the aquifer while very low values (<20 Ωm) in Enagi could be related to high saturation and higher salinity of the groundwater.

The groundwater prospects in the Kutigi-Enagi area are generally high with depth to aquifer lower at Kutigi (20 meters) relative to Enagi (30 meters). Drilled wells in these areas will produce prolific groundwater to boreholes at depth of 40 meters at Kutigi and Enagi respectively. The presence of pebbles in the clayey sand aquifers in Enagi is expected to produce a greater groundwater yield to boreholes here.

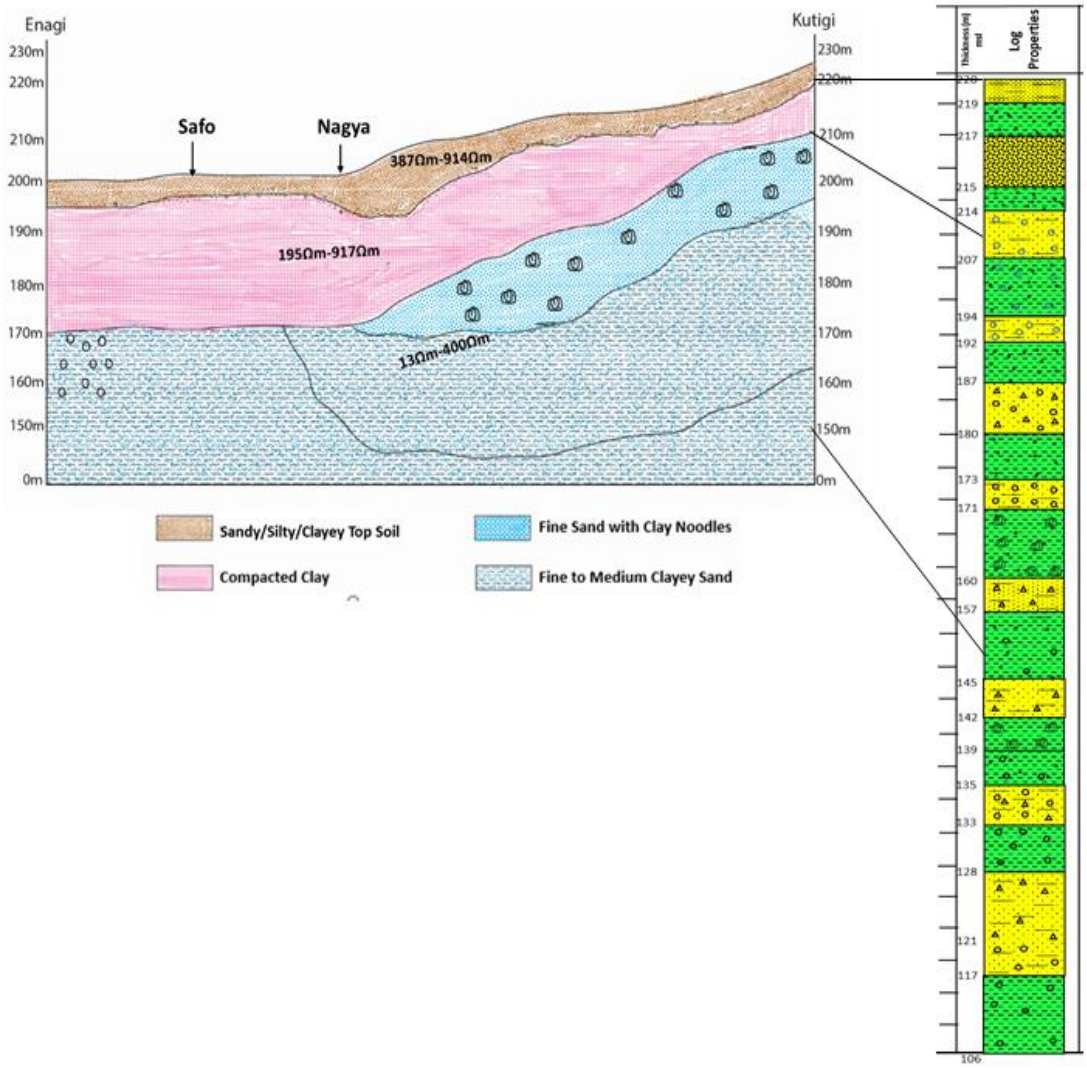

Figure 7: Geo-electric Section for the Study Area (Enagi to Kutigi) correlated with Kutigi borehole log

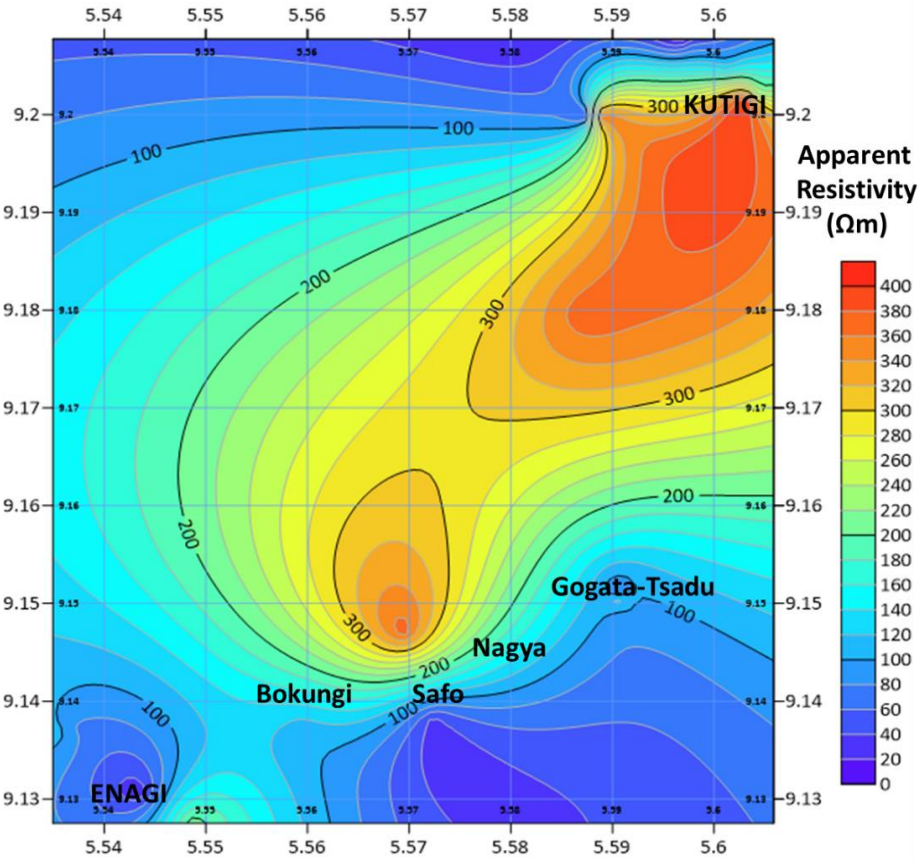

Figure 8: True aquifer Resistivity Map of the Study Area

CONCLUSION

Electrical resistivity tomography (ERT) and vertical electrical sounding (VES) were integrated to access the groundwater potential of Kutigi-Enagi region of the northern Bida Basin. These methods remain the most reliable and cost-effective methods for local scale groundwater exploration especially in Saharan Africa. The ERT is useful in understanding lateral variation of lithologies interpreted from their apparent resistivity values. This variation is important in identifying possible areas of groundwater recharge as well as lithologies that are aquiferous. The VES is reliable in collecting and interpreting lithologies with depth and relating them with their resistivity values and integrated with ERT to infer lateral variation. When VES and ERT data are systematically collected across several locations, they can provide quick understanding regarding the local and regional aquifer settings in an area.

The groundwater prospects in the area are generally high with aquifer depths between 20 meters and 30 meters. Properly constructed boreholes in these areas with depths of 40 meters will produce prolific groundwater.

ACKNOWLEDGEMENT

We thank the Tertiary Education Trust Fund (TETFund) for providing funding for the research through the Institutional Based Research (IBR) and Academic Staff Training and Development (AST&D) Intervention.

REFERENCES

- Adeleye, D. R. (1974). Sedimentology of the fluvial Bida Sandstones (Cretaceous), Nigeria. *Sediment Geology*, 12, 1-24.
- Aizebeokhai, A. P., Oyeyemi, K. D., & Joel, E. S. (2016). Groundwater potential assessment in a sedimentary terrain, Southwestern Nigeria. *Arab J. Geosci*, 9(496), 1-15. https://doi.org/10.1007/S12517-016-2524-5.
- Boubaya, D. (2017). Combining Resistivity and Aeromagnetic Geophysical Surveys for Groundwater Exploration in the Maghnia Plain of Algeria. *Journal of Geological Research*, 1 – 14. https://doi.org/10.1155/2017/1309053.
- Ewusi, A., Kuma, J. S., & Voigt, H. J. (2009). Utility of the 2-D multi-electrode resistivity imaging technique in groundwater exploration in the Voltaian Sedimentary Basin, Northern Ghana. *Natural Resources Research*, 18(4), 267-275. https://doi.org/10.1007/S11053-009-9102-4.
- Harini, P., Sahadevan, D. K, Das, I. C., Manikyamba, C., Durgaprasad, M., & Nandan, M. J. (2018). Regional Groundwater Assessment of Krishna River Basin Using Integrated GIS Approach. *Journal of the Indian Society of Remote Sensing*, 46(9), 1365-1377. https://doi.org/10.1007/S12524-018-0780-4.

- Hewaidy, A. G., El-Motaal, E. A., Sultan, A. S., Ramdan, T. A., El khafif A. A., & Soliman S. A. (2015). Groundwater exploration using resistivity and magnetic data at the northwestern part of the Gulf of Suez, Egypt. *Egyptian Journal of Petroleum*, 24, 255-263. http://dx.doi.org/10.1016/j.ejpe.2015.07.010.
- Holting, B., & Coldewey, W. G. (2019). *Hydrogeology*. Springer Textbooks in Earth Sciences, Geography and Environment. Springer-Verlag GmbH.
- Idris-Nda, A., Abubakar, S. I., Waziri, S. H., Dadi, M. I., & Jimada, A. M. (2014). Groundwater Development in a Mixed Geological Terrain: A Case Study of Niger State, Central Nigeria. *Water Resources Management*, 8, 77-87.
- Khaki, M., Yusoff, I & Islami, N. (2016). Electrical resistivity imaging and hydrochemical analysis for groundwater investigation in Kuala Langat, Malaysia. *Hydrological Science Journal*, 61(4), 751-762.
- Kogbe, C. A. Ajakaiye, D. E., & Matheis, G. (1983). Confirmation of rift structure along the Mid-Niger Valley, Nigeria. *Journal of African Earth Science*, 1, 127–131.
- Loke, M. H., & Barker, R. D. (1996). Rapid least-squares inversion of apparent resistivity pseudosections using a quasi-Newton method. *Geophysical Prospecting*, 44, 131-152.
- NurAmalina, M. K. A., Nordiana, M. M., Bery, A. A., Akmal Bin Anuar, M. N., Maslinda. U., Sulaiman, N., Saharudin, M. A., Hisham, H., Nordiana, A. N., & Taqiuddin, Z. M. (2017). Application of 2-D resistivity imaging and seismic refraction method in identifying the structural geological contact of sedimentary lithologies. *IOP Conf. Series: Earth and Environmental Science*, 1-7. https://doi.org/10.1088/1755-1315/62/1/012005.
- Nyagwambo, N. L. (2006). *Groundwater recharges estimation and water resources assessment in a tropical crystalline basement aquifer*. Balkema Publishers.
- Obaje, N. G. (2009). *Geology and mineral resources of Nigeria*. Springer-Verlag Berlin Heidelberg.
- Olabode, T. O., Eduvie, M. O., & Olaniyan, I. O. (2012). Evaluation of groundwater resources of the Middle Niger (Bida) Basin of Nigeria. *American Journal of Environmental Engineering*, 2(6), 166-173.
- Rahaman, M. A. O., Fadiya, S. L., Adekola, S. A., Coker, S. J., Bale, R. B., Olawoki, O. A., Omada, I. J., Obaje, N. G., Akinsanpe, O.T., Ojo, G. A., & Akande, W. G. (2019). A revised stratigraphy of the Bida Basin, Nigeria. *Journal of African Earth Sciences.* https://doi.org/10.1016/j.jafrearsci.2018.11.016.
- Rani, P. (2017). *Geophysical modeling for groundwater and soil contamination risk assessment*. [PhD Thesis, Università Degli Studi Di Napoli Federico II]. Università Degli Studi Di Napoli Federico II.
- Sikah, J. N., Aning, A. A., Danuor, S. K., Manu, E., & Okrah, C. (2016). Groundwater Exploration using 1D and 2D Electrical Resistivity Methods. *Journal of Environment and Earth Science*, 6(7), 55-63.
- Taylor, R., & Barrett, M. (1999). Urban Groundwater Development in Sub Saharan Africa. *25th WEDC Conference Proc., Integrated Development for Water Supply and Sanitation*. Addis Ababa, Ethiopia, 203-207.